Original Article

DOI: 10.5582/ddt.2022.01107

Cyclic AMP (cAMP)-dependent proteolysis of GATA6 by proteasome: Zinc-finger domain of GATA6 has signals for nuclear export and proteolysis, both of which are responsive to cAMP

Tomohisa Yamamoto[1,a], Takeshi Tsuge[1,b], Makoto Araki[2], Masatomo Maeda[1,*]

[1] Graduate School of Pharmaceutical Sciences, Osaka University, Suita, Osaka, Japan;
[2] Meiji Pharmaceutical University, Tokyo, Japan.

SUMMARY Transcription factor GATA6 stably expressed in Chinese hamster ovary (CHO)-K1 cells is exported from the nucleus to the cytoplasm and degraded there by proteasome upon treatment with dibutylyl-cyclic AMP (*db*cAMP), which is a membrane-permeable cyclic AMP (cAMP) analogue. The cAMP-dependent proteolysis of GATA6 was characterized by dissection of the GATA6 protein into a zinc-finger domain (Zf) and the surrounding region (ΔZf). These segments were separately expressed in CHO-K1 cells stably, and followed by treatment with *db*cAMP. The nuclear localized Zf was degraded by proteasome similarly to the full-length GATA6. Site-directed mutants of nuclear localizing signal (NLS) (^{345}RKRKPK^{350} → AAAAPK and AAAAPA) and closely related GATA4 showed the same behavior. Although nuclear-localized ΔZf was degraded by proteasome, the cytoplasmic-located ΔZf was resistant to proteolysis in contrast to the NLS mutants. We also searched for a potential NLS and nuclear export signal (NES) with computational prediction programs and compared the results with ours. All these results suggest that the amino acid sequence(s) of the Zf of GATA6 is responsive to cAMP-dependent nuclear export and proteolysis.

Keywords Cyclic AMP-dependent protein kinase, GATA DNA-binding protein, nuclear-cytoplasmic shuttling, regulated protein degradation, stable transfection, cJun N-terminal kinase

1. Introduction

Transcription factor GATA6 is an essential gene product (*1,2*), and is required for the development of endoderm and mesoderm in early embryos, and differentiation of these germ layers into specific tissue cells and unique gene expression in those differentiated cells have been examined (*3,4*). Actually, it is well known that mutations of the *GATA6* gene often cause congenital heart disease and pancreatic agenesis (*4*). Furthermore, it is claimed that GATA6 participates in tumorigenesis, although controversial findings as to the tumor suppressor function of GATA6 have been also reported (*5*). Thus, studies on the molecular properties of GATA6 are informative to understand the cause of the disease and to develop a strategy for its treatment.

There are six GATA family DNA-binding proteins in mammals, which recognize the canonical (A/T)GATA(A/G) motif (GATA-motif) in gene regulatory regions. Each member has a highly conserved zinc-finger domain (Zf) composed of tandem zinc-finger segments separated by 29 amino acid residues ($CX_2CX_{17}CX_2C$)-X_{29}-($CX_2CX_{17}CX_2C$) and a following basic region, but the surrounding region (ΔZf) shows sequence divergency (*6*). The carboxy (C)-terminal zinc-finger segment (C-finger) binds to the GATA-motif whereas the amino (N)-terminal zinc-finger segment (N-finger) interacts with the adjacent GATA-motif or with protein cofactors (*3,4*). Since the basic region following the C-finger further functions as a nuclear localization signal (NLS) (*3,4*), GATA proteins translated in the cytoplasm are immediately transported into the nucleus in both the native state and as exogenously expressed (*7-10*).

We have found that stably but not transiently expressed GATA6 is exported from the nucleus to the cytoplasm upon activation by cyclic AMP (cAMP)-dependent protein kinase (PKA) (*11*). Following the nuclear export mediated by Chromosome Region Maintenance 1 [CRM1, also known as Exportin-1 (XPO1)] (*12*), GATA6 is further degraded by proteasome (*11,12*). Although GATA6 remained stably in the nucleus in the presence of a proteasome inhibitor, proteasomal degradation of GATA6 is suggested to occur in the cytoplasm: activation of PKA stimulated degradation of

GATA6 when it was tethered on the cytoplasmic side of the endoplasmic reticulum membrane through the membrane anchoring domain of the sterol regulatory element-binding protein (SREBP) 2 (*13*). Furthermore, nuclear export and cytoplasmic degradation of GATA6 can be discriminated when stimulated on activation by cJun N-terminal kinase (JNK) since GATA6 is rapidly exported from the nucleus and then slowly degraded in the cytoplasm (*12*).

In this study, we focused on the Zf and ΔZf of GATA6 separately, and characterized their degradation induced by dibutylyl-cyclic AMP (*db*cAMP). Unveiling of the mechanism of sequestration of GATA6 from the nucleus could be helpful for manipulating the cellular localization of transcription factors from the viewpoint of therapeutics for diseases.

2. Materials and Methods

2.1. Construction of expression plasmids for human GATA6 (hGATA6) derivatives

The expression plasmid for the hGATA6 Zf (hZf) (Glu^{240}-Thr^{357}) (*14*) was constructed by the procedure shown in Figure S1 (*http://www.ddtjournal.com/action/getSupplementalData.php?ID=133*). From this plasmid, named pME-HA/FLAG-hZf, hZf was expressed as a fusion protein with amino-terminal human influenza hemagglutinin (HA) and FLAG tags.

To delete the Zf between S^{239} and T^{357} of S-type hGATA6 (*14*), *Dpn*I-mediated site-directed mutagenesis (*15*) was carried out: the mutant DNA was amplified by means of polymerase chain reaction (PCR) with primer pair dZfa/dZfs, PrimeSTAR HS DNA polymerase (TaKaRa, Kusatsu, Shiga, Japan), and pME-hGT1SMyc (*16*) as a template under the following conditions: 94°C 2 min, followed by 30 cycles of denaturation (94°C, 10 sec), annealing (68°C, 6 min), and extension (68°C, 6 min), and then post-incubation (72°C, 5 min). The reaction mixture was treated with *Dpn*I to degrade methylated parental DNA, and then transformed into *Escherichia coli* Top10F' (Invitrogen, Carlsbad, CA, USA). The resulting plasmid was named pME-hGT1S(ΔZf)Myc.

To construct an expression plasmid for NLS mutant 1 with Myc-tag (NLSmut1-Myc) [pME-hGT1S(NLSmut1)Myc], the plasmid template pME-hGT1SMyc was subjected to PCR with primer pair TYmut1s/TYmut1a and Pyrobest DNA polymerase (TaKaRa) [95°C 5 min, followed by 20 cycles of denaturation (94°C, 15 sec), annealing (55°C, 30 sec), and extension (72°C, 5 min)]. The product was digested with *Dpn*I and then introduced into *Eschericha coli* Top10F'. The ~400 base pair (bp) *Eco*RI-*Spe*I fragment with base-substitutions was inserted into the corresponding part of pME-hGT1SMyc. The expression plasmid for NLSmut2-Myc [pME-hGT1S(NLSmut2)Myc] was similarly constructed with primer pair TYmut2s/TYmut2a using pME-hGT1S(NLSmut1)Myc as a template.

DNA fragments were size-separated by agarose gel-electrophoresis [1%~2% (w/v)], and visualized with ethidium bromide. The sequence of the cloned DNA was determined by the dideoxy chain-termination method with sequence primers for the pME18S vector (*16*) and a BigDye™ terminator v3.1 Cycle Sequencing Kit (Applied Biosystems, Waltham, MA, USA), using an ABI PRISM™ 310 Genetic Analyzer (Applied Biosystems). The molecular biological methods for DNA manipulations were based on standard procedures as described in our previous study (*17*). The primers for PCR and sequencing are listed in Table S1 (*http://www.ddtjournal.com/action/getSupplementalData.php?ID=133*).

2.2. Cell culture and transfection of expression plasmids

Each plasmid construct was introduced into Cos-1 cells (ATCC, Manassas, VA, USA) by means of the diethylaminoethyl (DEAE)-dextran method (*17*) to verify expression of the recombinant protein. Cells were grown for two days in Dulbecco's modified Eagle medium (DMEM) (GIBCO BRL, Gaithersburg, MD, USA) supplemented with 7% fetal bovine serum (FBS) (GIBCO BRL) and antibiotics [100 units/mL benzylpenicillin (Wako, Osaka-city, Osaka, Japan), 100 μg/mL streptomycin sulfate (Wako), and 2.5 μg/mL fungison (GIBCO BRL)], and the transiently expressed proteins were detected immunologically as described in *2.3*.

Chinese hamster ovary (CHO)-K1 cells (*11*) were grown in Ham's F12 medium (GIBCO BRL) supplemented with FBS and antibiotics as above. Each expression plasmid for GATA6 derivatives was introduced into CHO-K1 cells by means of the calcium-phosphate method (*17*) together with phyg (*17*) in the ratio of 15:1 (w/w). Resistant colonies were selected in the presence of 200 μg/mL hygromycin (Wako). As for pME-HA/FLAG-hZf, pDsRed2-N1 (Clontech, Mountain View, CA, USA) was added in place of phyg and the transformants were selected in the presence of 100 μg/mL G418 (Sigma, St. Louis, MO, USA), the red fluorescence of *Discosoma*-derived protein DsRed being detected under a microscope (Olympus IX70, Olympus Corporation, Shinjuku-ku, Tokyo, Japan).

2.3. Detection of GATA proteins

Cells (1×10^6 cells in *Φ*10 cm dish) were cultured for 24 h, and then further incubated for 24 h in the presence or absence of 2 mM *db*cAMP (Sigma). Proteasome inhibitor benzyloxycarbonyl-L-leucyl-L-leucyl-L-norvalinal (MG115) (Peptide Institute Inc., Ibaraki, Osaka, Japan) (10 μM) was also added at 12 h before harvest. The postnuclear supernatant (cytoplasm) and nuclear protein

extract (nucleus) were prepared by the published method (*18*). Protein concentrations were determined with a Bio-Rad Protein Assay Kit (Hercules, CA, USA) (*19*) using bovine serum albumin (Fraction V) (Sigma) as a standard.

A protein sample (10 µg) was subjected to sodium dodecyl sulfate (SDS)-polyacrylamide gel-electrophoresis and Western blotting (*17*); the proteins were electro-blotted onto a Hybond-P Polyvinylidene Difluoride (PVDF) membrane (GE Healthcare, Chicago, IL, USA). The concentration of the separation gel was 7.5% (w/v) for Myc-tagged proteins, 15% (w/v) for hZf, and 10% (w/v) for others. Procedures for membrane blocking and washing were essentially the same as described previously (*13,17*).

The Myc-tagged human proteins and hZf were detected with peroxidase-linked mouse monoclonal antibodies; anti-c-Myc (MC045, Nacalai Tesque, Kyoto, Japan) (× 4,000 diluted) and ANTI-FLAG M2® (Sigma) (× 1,500 diluted), respectively. hGATA6 ΔZf (hΔZf)-Myc was further detected with rabbit site-specific polyclonal antibodies recognizing hGATA6 (Leu^{59}-Gln^{217}) (*18*) (× 1,000 diluted) as the first antibodies, second antibodies being horseradish peroxidase-linked donkey anti-rabbit immunoglobulin (Ig) (Amersham-Pharmacia Biotech, Burlington, MA, USA) (× 4,000 diluted). Chemiluminescence was detected with an ECL Western blotting kit (GE Healthcare) using Scientific Imaging film (KODAK, Rochester, NY, USA).

2.4. Chemicals

Restriction enzymes were obtained from New England Biolabs (Ipswich, MA, USA), Toyobo (Osaka-city, Osaka, Japan), and TaKaRa. The Klenow enzyme, T4 DNA ligase (Ligation Kit Ver.2.1) and Agarose-LE Classic Type were provided by TaKaRa. A GENECLEAN III Kit was obtained from BIO101 (La Jolla, CA, USA). Oligonucleotides were purchased from Gene Design Inc. (Ibaraki, Osaka, Japan). All other chemicals used were of the highest grade commercially available.

3. Results

3.1. Effect of amino terminal deletion of GATA6 on the response to *db*cAMP

Our previous studies demonstrated that not only full-length S-type hGATA6 (*18*) but also rat GATA6Δ50 (rGATA6Δ50) with deletion of the amino-terminal 50 residues (*11*) (hS-type and rΔ50, respectively, in Figure 1) were degraded by proteasome when CHO-K1 cells stably expressing either of these proteins were treated with *db*cAMP. We first evaluated further deletion of the amino terminal region between residues 72 and 131 of rat GATA6 (rGATA6) as to whether it is *db*cAMP-sensitive or not, the deleted protein being named rat GATA6Δ(1-50, 72-131) {[rGATA6Δ(1-50, 72-131)] and rΔ(1-50, 72-131) in Figure 1]}. This protein containing the Zf [Glu^{234}-Ala^{351}, residue numbers of rGATA6] is localized in the nucleus and degraded by proteasome in the presence of *db*cAMP when stably expressed in CHO-K1 cells (Figure S2, *http://www.ddtjournal.com/action/getSupplementalData.php?ID=133*), suggesting that the response to *db*cAMP is not attributable to the deleted segments.

Since earlier studies on other GATA proteins suggested that the Zf is responsible for their nuclear localization and DNA binding (*3,4*), we compared the Zf and ΔZf sequences of hGATA6 as to the response to *db*cAMP. These protein constructs (HA/FLAG-hZf, and hΔZf-Myc, respectively) are schematically shown in Figure 1 together with our previous ones (*11,18*).

3.2. Response of the Zf of hGATA6 to *db*cAMP

The Zf of hGATA6 (Glu^{240}-Thr^{357}) (*14*) was stably expressed in CHO-K1 cells as a fusion protein with an N-terminal HA/FLAG-tag (Figure 1 and Figure S1, *http://www.ddtjournal.com/action/getSupplementalData.php?ID=133*). As shown in Figure 2, HA/FLAG-hZf was localized in the nucleus of two isolated clones (Zf_8 and Zf_{20}), suggesting that the nuclear localization signal is present in the Zf. The amount of nuclear HA/FLAG-

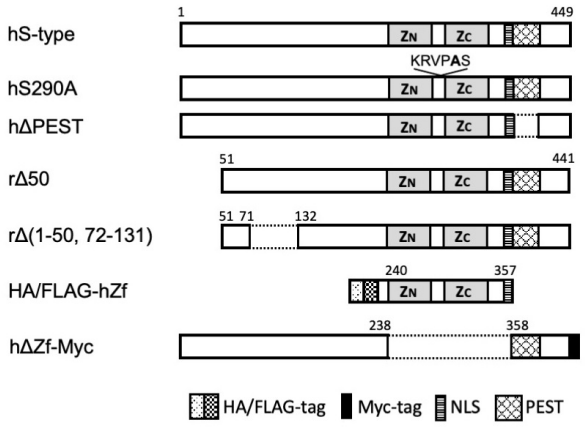

Figure 1. Schematic representation of GATA6 derivatives. The various GATA6 proteins expressed from plasmid constructs are schematically shown together with their names (left column). The sequences for rΔ50 (*11*) and rΔ(1-50, 72-131) (Figure S2) are of rat GATA6 origin, and those of the others human as indicated by adding a prefix "h". The expression plasmids for hS-type, hS290A and hΔPEST were described previously (*18*). The amino acid residue numbers of human and rat GATA6 are 449 and 441 (indicated above the boxes), respectively, based on the structure of S-type GATA6 (*14*). "Z_N" and "Z_C" indicating $(CX_2C)X_{17}(CX_2C)$ are the N-finger and C-finger, respectively, separated by 29 amino acid residues in the Zf. The positions of epitope tags (HA/FLAG-tag and Myc-tag), and potential NLS and peptide that is rich in proline, glutamic acid, serine and threonine (PEST) sequences (*18*) are shown schematically. The amino acid substitution (Ser to Ala) at position 290 (*18*) is also indicated in hS290A in bold.

hZf decreased when stable cells (both Zf_8 and Zf_{20}) were cultured in the presence of *db*cAMP, and this behavior was abolished in the presence of proteasome inhibitor MG115 (Figures 2A and 2B), indicating that the decrease of HA/FLAG-hZf in the cells is due to degradation by proteasome. The inhibition of its degradation would re-localize HA/FLAG-hZf into the nucleus due to the presence of NLS that functions dominantly. It was also confirmed that HA/FLAG-hZf was exclusively localized in the nucleus, *i.e.*, not found in the cytoplasm, of clone Zf_{20} (Figure 2C, right).

3.3. Response of the ΔZf of hGATA6 without the Zf to *db*cAMP

To compare the results for HA/FLAG-hZf, we stably expressed hΔZf-Myc without the Zf. The hΔZf-Myc was localized in both the nucleus and cytoplasm in all four clones isolated (Figure S3A, *http://www.ddtjournal.com/action/getSupplementalData.php?ID=133*). Interestingly, nuclear hΔZf-Myc decreased in the presence of *db*cAMP although that in the cytoplasm did not (Figure S3B, *http://www.ddtjournal.com/action/getSupplementalData.php?ID=133*). The behavior of one clone (ΔZf1-1) was examined further in detail, as shown in Figure 3: the corresponding bands to hΔZf-Myc have both N- and C-terminal regions since not only the C-terminal Myc-tag (Figure 3A) but also antibodies recognizing upstream Leu^{59}-Gln^{217} were reactive (Figure 3B). The decrease in the nuclear hΔZf-Myc was inhibited by the addition of MG115, indicating that it was degraded by proteasome.

An unexpected observation was that the cytoplasmic hΔZf-Myc was resistant to proteasome. A possible explanation is that association with other proteins (*20,21*) or the conformational state of an unusual artificial hΔZf-Myc, which may induce aggregation (*22,23*), could prevent most of the cytoplasmic hΔZf-Myc from gaining access to proteasome. Macromolecules smaller than ~40 kDa can passively diffuse through nuclear pores (*24*), and the molecular weight of hΔZf-Myc was calculated to be 32 k [GENETYX-MAC GENETIC INFORMATION PROCESSING SOFTWARE (GENETYX Corporation, Shibuya-ku, Tokyo, Japan)]. Thus, the monomeric hΔZf-Myc would freely enter the nucleus. Although some proteasome was found in the nucleus (*25*), we did not examine further whether the hΔZf-Myc is degraded in the nucleus or cytoplasm since expression of a fusion of hΔZf-Myc with the membrane domain of SREBP2 to fix hΔZf-Myc on the cytoplasmic side of the endoplasmic reticulum membrane (*13*) has not been successful.

3.4. Effect of substitution of the cluster of basic residues following the C-finger of hGATA6

We further examined whether the potential NLS of GATA6 affects the cAMP-dependent nuclear exit and proteolysis of GATA6. We substituted the Arg and Lys

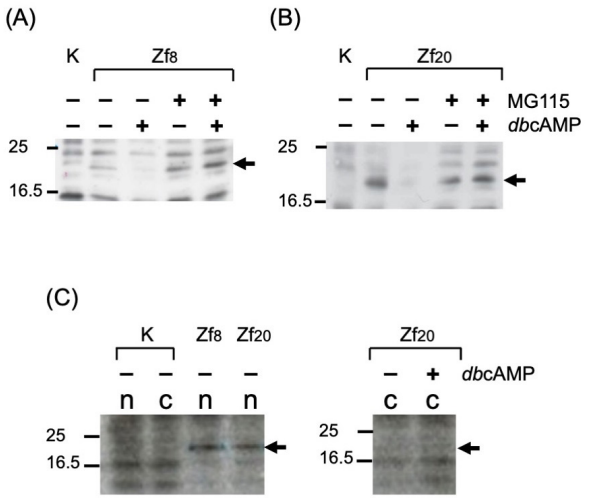

Figure 2. Behavior of HA/FLAG-hZf stably expressed in CHO-K1 cells in the presence of *db*cAMP. The expression plasmid for HA/FLAG-hZf (Figure S1) was stably introduced into CHO-K1 cells. Among 21 G418-resistant colonies, two clones (Zf_8 and Zf_{20}) were HA/FLAG-hZf protein-positive. Cells were cultured for 24 hr in the presence (+) or absence (–) of *db*cAMP and proteasome inhibitor MG115. The HA/FLAG-hZf protein in the nucleus was analyzed by means of Western blotting after SDS-polyacrylamide gel-electrophoresis as described under Materials and Methods **(A** and **B)**. The HA/FLAG-hZf protein in the nucleus (n) (Zf_8 and Zf_{20}) and cytoplasm (c) (Zf_{20}) was analyzed in **(C)**. Fractions prepared from CHO-K1 cells (K) were used as negative controls. The values on the left side are molecular weights ($\times 10^{-3}$). Arrows at the right indicate the position of HA/FLAG-hZf.

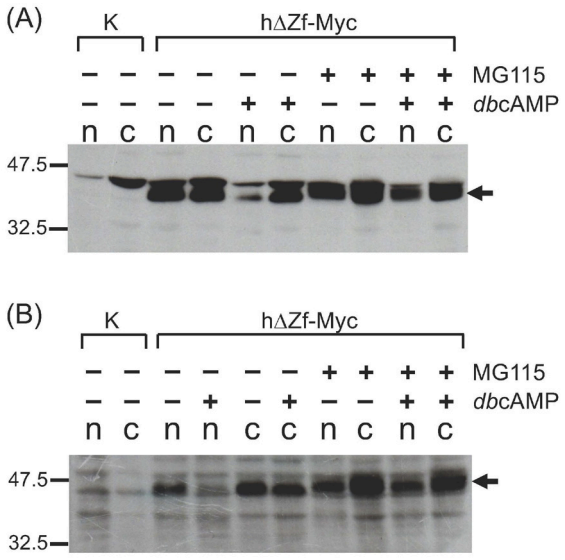

Figure 3. Behavior of hΔZf-Myc stably expressed in CHO-K1 cells in the presence of *db*cAMP. A stable clone (ΔZf1-1, see Figure S3) that expresses hΔZf-Myc was cultured in the presence (+) or absence (–) of *db*cAMP and MG115. The hΔZf-Myc in the nucleus (n) and cytoplasm (c) was detected by Western blotting after SDS-polyacrylamide gel-electrophoresis. Fractions prepared from CHO-K1 cells (K) were used as negative controls. The values on the left side are molecular weights (x 10^{-3}). Arrows on the right indicate the position of hΔZf-Myc. **(A)** Peroxidase-linked mouse monoclonal anti-c-Myc was used. **(B)** Rabbit site-specific polyclonal antibodies recognizing hGATA6 (Leu^{59}-Gln^{217}) as the first antibodies, and horseradish peroxidase-linked donkey anti-rabbit Ig as the second antibodies were used.

residues, which are clustered downstream of the C-finger (*3*). This cluster is also predicted to be a NLS by all the prediction programs available (Table S2 [A], *http://www.ddtjournal.com/action/getSupplementalData.php?ID=133*). In the two mutants, NLSmut1-Myc and NLSmut2-Myc, the sequence ^{345}RKRKPK^{350} is ^{345}AAAAPK^{350} and ^{345}AAAAPA^{350}, respectively (Figure 4A). When these mutant proteins were stably expressed in CHO-K1 cells, they were distributed in both the nucleus and cytoplasm. Furthermore, both nuclear and cytoplasmic NLS-mutant proteins were degraded by proteasome in the presence of *db*cAMP since MG115 inhibited their decrease (Figure 4B and 4C), in contrast to hΔZf-Myc.

All these results suggest that the four consecutive basic residues function as the NLS, although nuclear import of the mutant proteins was not inhibited completely. Such behavior could be ascribed to the following possibilities: (*i*) another NLS also participates in the nuclear import of GATA6, and/or (*ii*) a nuclear export signal (NES) without the RKRKPK sequence is unveiled, although such NLS and NES would have weak activity. In chicken GATA1, the RNRKVS sequence present at an identical position to GATA6 (Figure 5) is required for specific DNA-binding of GATA1 to the GATA-motif (*26*), suggesting that the present NLS mutants would have low affinity as to the GATA-motif and thus would be easily excreted from the nucleus in the absence of *db*cAMP.

The results in Figure 2 and Figure 4 suggested that the Zf is important for *db*cAMP-dependent degradation of GATA6. Consistent with this notion, we further demonstrated that nuclear GATA4, which has a highly conserved Zf [88% and 97% of the residues are identical and conservative, respectively, between rat GATA4 (rGATA4) and rGATA6 (Figure 5) (*6*)], similarly disappeared in the presence of *db*cAMP (Figure S4, *http://www.ddtjournal.com/action/getSupplementalData.php?ID=133*).

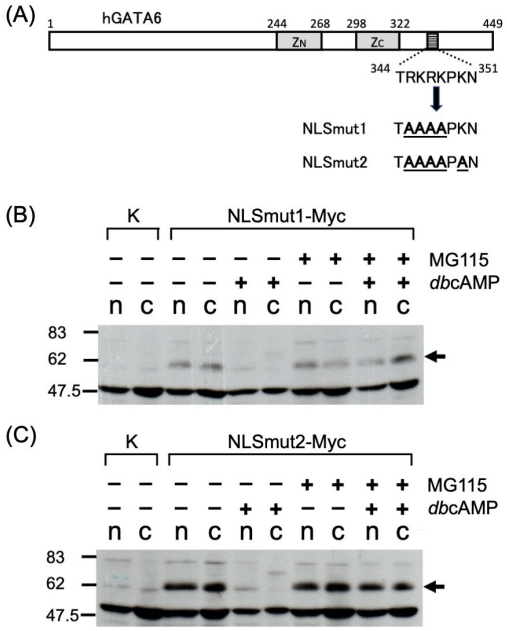

Figure 4. Effects of substitution of basic residues in the NLS. S-type hGATA6 (449 residues) is schematically shown in **(A)**. The C-terminal Myc-tag is omitted in the figure. The N-finger and C-finger are indicated by Z_N and Z_C, respectively. Amino acid residue numbers are shown above the box. Basic residues (Arg and Lys) in the potential NLS of GATA6 were substituted with Ala residues in the two mutant proteins (NLSmut1 and NLSmut2), as underlined. Expression plasmids for two mutants [pME-hGT1S(NLSmut1)Myc and pME-hGT1S(NLSmut2)Myc] were constructed as described under Materials and Methods. They were introduced into CHO-K1 cells and hygromycin-resistant colonies (15 and 4, respectively) were isolated. Among them, four and one clones expressed mutant GATA6. Clones (one of the positive clones for each mutant) were cultured in the presence (+) or absence (–) of *db*cAMP and MG115. The NLSmut1-Myc and NLSmut2-Myc in the nucleus (n) and cytoplasm (c) were detected by Western blotting after SDS-polyacrylamide gel-electrophoresis [**(B)** and **(C)**, respectively]. Fractions prepared from CHO-K1 cells (K) were used as negative controls. The values on the left side are molecular weights ($\times 10^{-3}$). Arrows on the right indicate the positions of NLSmut1-Myc and NLSmut2-Myc, respectively.

4. Discussion

We have shown in this and our previous studies (*11-13,18*) that nuclear-localized GATA6 is exported into the cytoplasm upon *db*cAMP-treatment. A GATA factor (GtaC) of *Dictyostelium discoideum* moves from the nucleus to the cytoplasm in response to cAMP since its NLS is neutralized upon input of the cAMP signal (*27*). Although the exported GtaC re-enters the nucleus, the GATA6 is degraded in the cytoplasm (*13*). However, conservation of the phenomena that both GATA proteins are exported from the nucleus to the cytoplasm in response to the cAMP signal is interesting, although they are evolutionally distant.

Since nuclear export of GATA6 depends on CRM1 (*12*), the leucin-rich NES (*28*) may participate in the process. The three Leu residues in the sequence ^{47}SVLGLSYLQG^{56} of mouse GATA4 (mGATA4) are crucial for its nuclear export (*29*). However, the corresponding sequence of hGATA6 (^{50}SMLPGLPYHLQG^{61}) (*14*) is located outside of the Zf. When we searched for candidate NES sequences in the Zf (Table S2, *http://www.ddtjournal.com/action/getSupplementalData.php?ID=133*), the sequence between Asn^{312} and Met^{337} including part of the C-finger was predicted with all three tools used. Thus, this region could be the next target of mutagenesis study as to whether it participates in the *db*cAMP-dependent nuclear export of GATA6.

The low steady-state level of tumor suppressor p53 under normal conditions is maintained through nuclear export, which results in its cytoplasmic degradation by proteasome. However, its CRM1-dependent export is complex: the mouse double minute 2 (MDM2) protein associates with p53 and the NES of

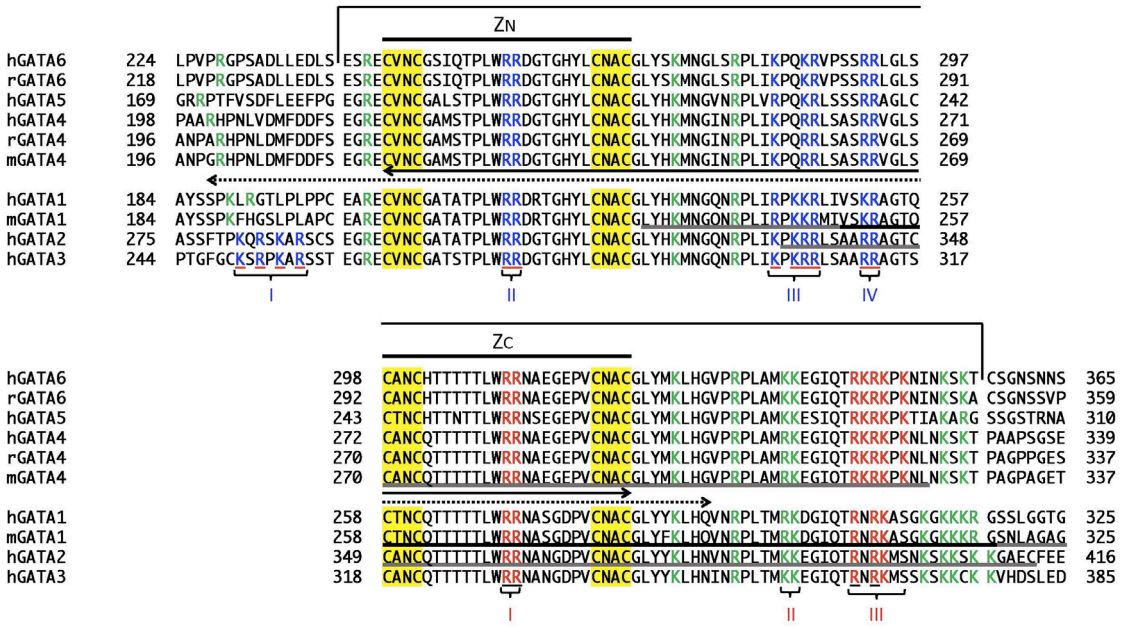

Figure 5. Sequence comparison of the Zfs of mammalian GATA proteins. Parts of the amino acid sequences of mammalian GATA proteins (h, human; r, rat; m, mouse) are aligned and shown as single letters. The Zf is indicated by a square bracket, and zinc-finger segments (CX_2C) $X_{17}(CX_2C)$ areindicated by Z_N (N-finger) and Z_C (C-finger) above, respectively. The accession numbers of the National Center for Biotechnology Information (NCBI) reference sequences are NM_005257 (hGATA6) (*14*), NM_019185 (rGATA6) (*14*), NM_080473 (hGATA5), NM_001308093 (hGATA4), NM_144730 (rGATA4) (*6*), NM_008092 (mGATA4), NM_002049 (hGATA1), NM_008089 (mGATA1), NM_001145661 (hGATA2), and NM_001002295 (hGATA3). Conserved basic residues (R and K) suggested to be NLS of hGATA3 (*35*) are indicated by blue letters, those of GATA4 (*29*) and GATA6 (present study) by red letters, and other conserved residues (including partially) by green letters. In mGATA4, which is more closely related to GATA6 compared to GATA1, 2, and 3, clusters I and III (indicated in red) are simultaneously required for nuclear localization of the full-length mGATA4, and R^{282}, R^{283}, R^{317} and R^{319} are crucial in the clusters (*29*). Furthermore, the minimum sequence imported into the nucleus is fragment C^{270}-L^{324} (underlined in grey color), although fragment C^{216}-C^{294} (underlined with arrowheads) and the G^{199}-G^{302} deletion (dotted underlined with arrowheads) were not imported (*9,29*), which is consistent with the importance of both clusters I and III (red). In mGATA1, the construct without either the N-finger (A^{197}-H^{232}) or C-finger (Q^{256}-Y^{285}), or deletion of K^{308}-S^{413} or ^{312}KGKKK^{316}, and fragment L^{230}-V^{336} or V^{250}-G^{318} (underlined in grey and overlapped portions in bold black) were imported into the nucleus, suggesting that the ^{243}RPKKR^{247} and ^{312}KGKKK^{316} sequences may independently direct this nuclear localization (*7,39*). In hGATA2, fragment P^{335}-C^{413} (underlined in grey) was transported into the nucleus (*7*). In contrast to these GATA proteins, combined mutations of basic residues in all four clusters (I - IV indicated by blue) disrupt nuclear localization of full-length hGATA3 (*35*), although the N-finger plus its N-terminal and C-terminal flanking sequences (C^{249}-A^{311}) is enough for localization in the nucleus (*8,35*). However, a truncation mutation (A^{311}→Stop) without the C-terminal sequence from cluster IV disrupts nuclear localization, suggesting that its C-terminal sequence from A^{311} might also affect the nuclear import mechanism (*35*). Furthermore, essential residues identified in mGATA4 (R^{282}, R^{283}, R^{317} and R^{319}) (*29*) could not function as the NLS in hGATA3 (R^{330}, R^{331}, R^{365} and R^{367} located at conserved positions) (*35*).

MDM2 is utilized for the nuclear export of p53 (*30*), while the intrinsic p53 NES seems to be sufficient for its export (*31*). Furthermore, the Jun activation-domain binding protein 1 (Jab1), as a component of Constitutive photomorphogenesis 9 (COP9) signalosome (CSN), stimulates CSN-associated kinase, resulting in phosphorylation of p53 and its nuclear export (*32*). Although curcumin inhibits CSN-associated kinase and the nuclear export of p53, this inhibitor did not affect the nuclear export of GATA6 (not shown).

The A-kinase and ubiquitin participates in *db*cAMP-induced nuclear export and degradation of GATA6 (*11,18*). Since GATA6 is not phosphorylated or ubiquitinqted during the process, it seems likely that the escort protein, which has a NES and is subjected to phosphorylation and ubiquitination, facilitates the nuclear export and degradation of GATA6. A p27 protein designated the cyclin-dependent kinase inhibitory protein-1 ($p27^{Kip1}$), which has no apparent NES, is exported from the nucleus to the cytoplasm through binding to Jab1, whose NES binds to CRM1, and then the exported $p27^{Kip1}$ is subjected to ubiquitin-dependent degradation by cytoplasmic proteasome. However, the Jab1 binding motif (-$DX_{21}LX_9N$-) identified in $p27^{Kip1}$ (*33*) could not be found in GATA6. Analysis of the altered genes of the mutants where GATA6 could not be exported in the presence of *db*cAMP or stably located in the nucleus even in the presence of *db*cAMP (*34*) might be helpful for identifying such escort proteins and provide their clues.

GATA6 as well as other GATA family members are localized in the nucleus after translation in the cytoplasm due to the presence of dominant NLS (*3,4*). The present results suggest that the classical monopartite ^{345}RKRK^{348} sequence (*24,28*) in hGATA6 contributes significantly as an NLS. Our NLS mutants and hΔZf-Myc are distributed in both the nucleus and cytoplasm, which could be explained by that the weak NES or NLS in these mutant

sequences would function. Although mutant proteins were distributed in both fractions in similar experiments to identify the NLS (*29,35*), it must be further mentioned that the amounts of cytoplasmic protein are more than twice higher than that in the nucleus (*36*), indicating that the mutant proteins are mainly distributed in the cytoplasm.

To explain the nuclear localization of our mutant proteins, we examined whether there are further putative classical NLS motifs in the S-type hGATA6 sequence or not (Table S2, *http://www.ddtjournal.com/action/getSupplementalData.php?ID=133*). However, only sequences containing ^{345}RKRK^{348} are predicted. Furthermore, visual examination did not reveal a classical bipartite NLS (*37*) or non-classical PY-NLS (*38*). One predicted sequence between Pro^{332} and Ser^{362} containing several basic residues together with ^{345}RKRK^{348} (Table S2, *http://www.ddtjournal.com/action/getSupplementalData.php?ID=133*) may be considered in the future study as to whether it is a more active NLS or not.

For nuclear import of mGATA4, two clusters of basic residues (^{282}RR^{283} and ^{317}RKRKPK^{322}) are simultaneously required for nuclear localization of full-length mGATA4 (Figure 5) (*29*). However, our study demonstrated that only ^{345}RKRK^{348} is enough as the NLS of full-length hGATA6. We also demonstrated that the mutant carrying the ^{310}AA^{311} and ^{345}AAAAPA^{350} sequences showed essentially the same behavior as that of NLSmut1 and NLSmut2 (not shown). As for the NLSs of GATA family proteins, the basic region following each C-finger is proposed to carry the signal (*3,4*). However, various reports are not consistent (see legend to Figure 5), although it has been demonstrated that the highly conserved Zfs of GATA proteins (Figure 5) participate in their nuclear import (*7-9,29,35,39*). Such differences could be ascribed to that (*i*) subtle amino-acid variations in the Zf and/or the unique sequences outside of the Zf affect the mode of interaction with importins, (*ii*) transformed cells are used, which frequently express virus antigen (*7,8,35,39*), as it was demonstrated that simian virus 40 (SV40) large T-antigen having a strong NLS escorts other proteins into the nucleus (*40*), and/or (*iii*) most of the experiments were carried out with a transient expression system (*7-9,29,35,39*), in which excess amounts of import substrates are produced in a short time, which often induces an abnormal cellular response (*41,42*).

It is well known that proteolytic degradation of GATA proteins participates in normal and abnormal cell differentiation: the expression levels of GATA2 and GATA3 are regulated *via* ubiquitin-dependent degradation upon hematopoietic and T-cell differentiation, and their phosphorylation by cyclin-dependent kinase 1 and 2 (CDK1 and CDK2), respectively, is required for recognition by S-phase kinase-associated protein 1 (Skp), Cullin, and F-box (SCF)-type E3 ubiquitin ligase (*43,44*), although intracellular degradation-sites of GATA2 and GATA3 have not been determined. Furthermore, GATA1 bacame susceptible to caspase3 upon sequestration of heat shock protein 70 (HSP70), resulting in differentiation impairment of erythropoiesis (*45*). However, extracellular signal-regulated kinase (ERK) [mitogen-activated protein kinase (MAPK)] rather stabilizes GATA1 and GATA3 (*44,46*).

In contrast, the responses of GATA6 and GATA4 to *db*cAMP are evoked by A-kinase (*11*). JNK further participates between proteasomal degradation of GATA6 and activation of A-kinase by *db*cAMP (*12*). Since JNK is known as a stress kinase (*47*), prolonged incubation with *db*cAMP and/or successive A-kinase activation would induce a stress response as a feed-back mechanism. Elucidation of such a cellular pathway will provide a hint to cure cancers of the gastrointestinal tract and hypertrophic cardiomyopathy, in which increased expression of GATA6 and GATA4, respectively, is likely to be causative of these diseases (*5,48,49*). Development of specific peptides inhibiting or accelerating the binding of GATA6 and GATA4 through their NLS or NES to importin families (*47*) could be useful for depleting nuclear GATA proteins. Another approach to their cellular depletion would be the finding of small-molecular protein degraders (*50*) that glue target GATA6 and GATA4 to E3 ubiquitin ligases.

Acknowledgements

We thank Dr. Kazuaki Ohashi for construction of the expression plasmids. We also thank Mr. Ken Miura for transfection of the GATA4 expression plasmid.

Funding: This work was supported in part by the JSPS (Grant-in-Aid for Scientific Research (B), 14370744, to M.M.).

Conflict of Interest: The authors have no conflicts of interest to disclose.

References

1. Morrisey EE, Tang Z, Sigrist K, Lu MM, Jiang F, Ip HS, Parmacek MS. GATA6 regulates HNF4 and is required for differentiation of visceral endoderm in the mouse embryo. Genes Dev. 1998; 12:3579-3590.
2. Koutsourakis M, Langeveld A, Patient R, Beddington R, Grosveld F. The transcription factor GATA6 is essential for early extraembryonic development. Development. 1999; 126:723-732.
3. Molkentin JD. The zinc finger-containing transcription factors GATA-4, -5, and -6: ubiquitously expressed regulators of tissue-specific gene expression. J Biol Chem. 2000; 275:38949-38952.
4. Tremblay M, Sanchez-Ferras O, Bouchard M. GATA transcription factors in development and disease. Development. 2018; 145:dev164384.

5. Deng X, Jiang P, Chen J, Li J, Li D, He Y, Jiang Y, Zhang Y, Xu S, Li X, Wang S, Tian F. GATA6 promotes epithelial-mesenchymal transition and metastasis through MUC1/β-catenin pathway in cholangiocarcinoma. Cell Death Dis. 2020; 11:860.
6. Maeda M, Kubo K, Nishi T, Futai M. Roles of gastric GATA DNA-binding proteins. J Exp Biol. 1996; 199:513-520.
7. Visvader JE, Crossley M, Hill J, Orkin SH, Adams JM. The C-terminal zinc finger of GATA-1 or GATA-2 is sufficient to induce megakaryocytic differentiation of an early myeloid cell line. Mol Cell Biol. 1995; 15:634-641.
8. Yang Z, Gu L, Romeo P-H, Bories D, Motohashi H, Yamamoto M, Engel JD. Human GATA-3 *trans*-activation, DNA-binding, and nuclear localization activities are organized into distinct structural domains. Mol Cell Biol. 1994; 14:2201-2212.
9. Morrisey EE, Ip HS, Tang Z, Parmacek MS. GATA-4 activates transcription *via* two novel domains that are conserved within the GATA-4/5/6 subfamily. J Biol Chem. 1997; 272:8515-8524.
10. Gillio-Meina C, Hui YY, LaVoie HA. GATA-4 and GATA-6 transcription factors: expression, immunohistochemical localization, and possible function in the porcine ovary. Biol Reprod. 2003; 68:412-422.
11. Nakagawa R, Sato R, Futai M, Yokosawa H, Maeda M. Gastric GATA-6 DNA-binding protein: proteolysis induced by cAMP. FEBS Lett. 1997; 408:301-305.
12. Ushijima H, Maeda M. cAMP-dependent proteolysis of GATA-6 is linked to JNK-signaling pathway. Biochem Biophys Res Commun. 2012; 423:679-683.
13. Tsuge T, Uetani K, Sato R, Ohashi-Kobayashi A, Maeda M. Cyclic AMP-dependent proteolysis of GATA-6 expressed on the intracellular membrane. Cell Biol Int. 2008; 32:298-303.
14. Yoshida T, Sato R, Mahmood S, Kawasaki S, Futai M, Maeda M. GATA-6 DNA binding protein expressed in human gastric adenocarcinoma MKN45 cells. FEBS Lett. 1997; 414:333-337.
15. Fisher CL, Pei GK. Modification of a PCR-based site-directed mutagenesis method. Biotechniques. 1997; 23:570-574.
16. Takada K, Obayashi K, Ohashi K, Ohashi-Kobayashi A, Nakanishi-Matsui M, Maeda M. Amino-terminal extension of 146 residues of L-type GATA-6 is required for transcriptional activation but not for self-association. Biochem Biophys Res Commun. 2014; 452:962-966.
17. Yokura-Yamada Y, Araki A, Maeda M. Ectopic expression of Id1 or Id3 inhibits transcription of the GATA-4 gene in P19CL6 cells under differentiation condition. Drug Discov Ther. 2021; 15:189-196.
18. Ishida A, Iijima R, Kobayashi A, Maeda M. Characterization of cAMP-dependent proteolysis of GATA-6. Biochem Biophys Res Commun. 2005; 332:976-981.
19. Bradford MM. A rapid and sensitive method for the quantitation of microgram quantities of protein utilizing the principle of protein-dye binding. Anal Biochem. 1976; 72:248-254.
20. Hunt T. Cytoplasmic anchoring proteins and the control of nuclear localization. Cell. 1989; 59:949-951.
21. Pratt WB, Welsh MJ. Chaperone functions of the heat shock proteins associated with steroid receptors. Semin Cell Biol. 1994; 5:83-93.
22. Kaganovich D, Kopito R, Frydman J. Misfolded proteins partition between two distinct quality control compartments. Nature. 2008; 454:1088-1095.
23. Balchin D, Hayer-Hartl M, Hartl FU. *In vivo* aspects of protein folding and quality control. Science. 2016; 353: aac4354.
24. Marfori M, Mynott A, Ellis JJ, Mehdi AM, Saunders NFW, Curmi PM, Forwood JK, Bodén M, Kobe B. Molecular basis for specificity of nuclear import and prediction of nuclear localization. Biochim Biophys Acta. 2011; 1813:1562-1577.
25. von Mikecz A. The nuclear ubiquitin-proteasome system. J Cell Sci. 2006; 119:1977-1984.
26. Omichinski JG, Clore GM, Schaad O, Felsenfeld G, Trainor C, Appella E, Stahl SJ, Gronenborn AM. NMR structure of a specific DNA complex of Zn-containing DNA binding domain of GATA-1. Science. 1993; 261:438-446.
27. Cai H, Katoh-Kurasawa M, Muramoto T, Santhanam B, Long Y, Li L, Ueda M, Iglesias PA, Shaulsky G, Devreotes PN. Nucleocytoplasmic shuttling of a GATA transcription factor functions as a development timer. Science. 2014; 343:1249531.
28. Cautain B, Hill R, de Pedro N, Link W. Components and regulation of nuclear transport processes. FEBS J. 2015; 282:445-462.
29. Philips AS, Kwok JC, Chong BH. Analysis of the signals and mechanisms mediating nuclear trafficking of GATA-4: loss of DNA binding is associated with localization in intranuclear speckles. J Biol Chem. 2007; 282:24915-24927.
30. Freedman DA, Levine AJ. Nuclear export is required for degradation of endogenous p53 by MDM2 and human papillomavirus E6. Mol Cell Biol. 1998; 18:7288-7239.
31. Stommel JM, Marchenko ND, Jimenez GS, Moll UM, Hope TJ, Wahl GM. A leucine-rich nuclear export signal in the p53 tetramerization domain: regulation of subcellular localization and p53 activity by NES masking. EMBO J. 1999; 18:1660-1672.
32. Lee EW, Oh W, Song HP, Kim WK. Phosphorylation of p53 at threonine 155 is required for Jab1-mediated nuclear export of p53. BMB Rep. 2017; 50:373-378.
33. Tomoda K, Kubota Y, Arata Y, Mori S, Maeda M, Tanaka T, Yoshida M, Yoneda-Kato N, Kato J. The cytoplasmic shuttling and subsequent degradation of $p27^{Kip1}$ mediated by Jab1/CSN5 and the COP9 signalosome complex. J Biol Chem. 2002; 277:2302-2310.
34. Maeda M, Ishida, A, Ni L, Kobayashi A. Isolation of CHO-K1 clones defective in cAMP-dependent proteolysis, as determined by the stability of exogenously expressed GATA-6. Biochem Biophys Res Commun. 2005; 329:140-146.
35. Gaynor KU, Grigorieva IV, Allen MD, Esapa CT, Head RA, Gopinath P, Christie PT, Nesbit MA, Jones JL, Thakker RV. GATA3 mutations found in breast cancers may be associated with aberrant nuclear localization, reduced transactivation and cell invasiveness. Horm Canc. 2013; 4:123-139.
36. Shaiken TE, Opekun AR. Dissecting the cells to nucleus, perinucleus and cytosol. Sci Rep. 2014; 4:4923.
37. Kosugi S, Hasebe M, Matsumura N, Takashima H, Miyamoto-Sato E, Tomita M, Yanagawa H. Six classes of nuclear localization signals specific to different binding grooves of importin α. J Biol Chem. 2009; 284:478-485.
38. Lee BJ, Cansizoglu AE, Süel KE, Louis TH, Zhang Z, Chook YM. Rules for nuclear localization sequence

recognition by karyopherin β2. Cell. 2006; 126:543-558.
39. Shimizu R, Takahashi S, Ohneda K, Engel JD, Yamamoto M. *In vivo* requirements for GATA-1 functional domains during primitive and definitive erythropoiesis. EMBO J. 2001; 20:5250-5260.
40. Shaulsky G, Goldfinger N, Ben-Ze'ev A, Rotter V. Nuclear accumulation of p53 protein is mediated by several nuclear localization signals and plays a role in tumorigenesis. Mol Cell Biol. 1990; 10:6565-6577.
41. Kobayashi A, Kasano M, Maeda T, Hori S, Motojima K, Suzuki M, Fujiwara T, Takahashi E, Yabe T, Tanaka K, Kasahara M, Yamaguchi Y, Maeda M. A half-type ABC transporter TAPL is highly conserved between rodent and man, and the human gene is not responsive to interferon-γ in contrast to TAPl and TAP2. J Biochem. 2000; 128:711-718.
42. Kamakura A, Fujimoto Y, Motohashi Y, Ohashi K, Ohashi-Kobayashi A, Maeda M. Functional dissection of transmembrane domains of human TAP-like (ABCB9). Biochem Biophys Res Commun. 2008; 377:847-851.
43. Nakajima T, Kitagawa K, Ohhata T, Sakai S, Uchida C, Shibata K, Minegishi N, Yumimoto K, Nakayama KI, Masumoto K, Katou F, Niida H, Kitagawa M. Regulation of GATA-binding protein 2 levels *via* ubiquitin-dependent degradation by Fbw7: involvement of cyclin B-cyclin-dependent kinase 1-mediated phosphorylation of Thr^{176} in GATA-binding protein 2. J Biol Chem. 2015; 290:10368-10381.
44. Kitagawa K, Shibata K, Matsumoto A, Matsumoto M, Ohhata T, Nakayama KI, Niida H, Kitagawa M. Fbw7 targets GATA3 through cyclin-dependent kinase 2-dependent proteolysis and contributes to regulation of T-cell development. Mol Cell Biol. 2014; 34:2732-2744.
45. Frisan E, Vandekerckhove J, de Thonel A, *et al*. Defective nuclear localization of Hsp70 is associated with dyserythropoiesis and GATA-1 cleavage in myelodysplastic syndromes. Blood. 2012; 119:1532-1542.
46. Han X, Zhang J, Peng Y, Peng M, Chen X, Chen H, Song J, Hu X, Ye M, Li J, Sankaran VG, Hillyer CD, Mohandas N, An X, Liu J. Unexpected role for $p19^{INK4d}$ in posttranscriptional regulation of GATA1 and modulation of human terminal erythropoiesis. Blood. 2017; 129:226-237.
47. Flores K, Yadav SS, Katz AA, Seger R. The nuclear translocation of mitogen-activated protein kinases: molecular mechanisms and use as novel therapeutic target. Neuroendocrinology. 2019; 108:121-131.
48. Kawasaki Y, Matsumura K, Miyamoto M, Tsuji S, Okuno M, Suda S, Hiyoshi M, Kitayama J, Akiyama T. REG4 is a transcriptional target of GATA6 and is essential for colorectal tumorigenesis. Sci Rep. 2015; 5:14291.
49. Katanasaka Y, Suzuki H, Sunagawa Y, Hasegawa K, Morimoto T. Regulation of cardiac transcription factor GATA4 by post-transcriptional modification in cardiomyocyte hypertrophy and heart failure. Int Heart J. 2016; 57:672-675.
50. Ito T, Yamaguchi Y, Handa H. Exploiting ubiquitin ligase cereblon as a target for small-molecule compounds in medicine and chemical biology. Cell Chem Biol. 2021; 28:987-999.

Received November 25, 2022; Revised January 12, 2023; Accepted January 26, 2023.

Present Address: [a] Japan Tobacco Inc. Central Pharmaceutical Research Institute, [b] Corporate Communications Dept. Corporate Strategy Div. SHIONOGI & CO., LTD., Japan.

**Address correspondence to:*
Masatomo Maeda, Graduate School of Pharmaceutical Sciences, Osaka University, Yamada-oka, Suita, Osaka 565-0871, Japan.
E-mail: m.maeda.d5h@osaka-u.ac.jp

Released online in J-STAGE as advance publication February 4, 2023.